

DETERMINATION OF THE CRYSTAL STRUCTURE OF HYDROBORACITE $\text{CaMg}[\text{B}_3\text{O}_4(\text{OH})_3]_2 \cdot 3\text{H}_2\text{O}$

I. M. Rumanov and A. Ashirov

Institute of Crystallography, Academy of Sciences, USSR
Translated from *Kristallografiya*, Vol. 8, No. 6,
pp. 828-845, November-December, 1963
Original article submitted July 20, 1963

Hydroboracite is monoclinic; the cell has parameters $a = 11.71$, $b = 6.69$, $c = 8.20$ Å, $\beta = 102^\circ 40'$ and contains two formula units $\text{CaMgB}_6\text{O}_{11} \cdot 6\text{H}_2\text{O}$. The space group is $C_{2h}^4 = P2/c$.

The Ca and Mg atoms have been located from $P(u, v)$ projections and from weighted Patterson projections $C_2(u, v)$ and $S_2(u, v)$. The coordinates of the other 12 atoms in the asymmetric part of the cell have been determined by partial Fourier syntheses computed from structure factors having indices of a specific type, i.e., from syntheses of increased (one-color or black-and-white) symmetry. Use has also been made of partial syntheses constructed for reflections of zero experimental intensity, whose Fourier coefficients were computed from the positions of the previously located Ca and Mg atoms. The structure has been refined from a series of phase-weighted and ordinary electron-density projections. Hydrogen bonds have been detected by analysis of the distances between oxygen atoms.

Hydroboracite contains infinite chains $[\text{B}_3\text{O}_4(\text{OH})_3]_n^{-2n}$, which extend along \underline{c} ; the BO_3 triangle is a distinctive element in these, and it occurs with two boron-oxygen tetrahedra linked into a ring by common vertices. (Such chains have also been found in colemanite.) The Mg cations lie at the centers of oxygen octahedra, which are joined via common H_2O vertices into $[\text{Mg}(\text{OH})_2 \cdot 3\text{H}_2\text{O}]_n$ chains, which also extend along \underline{c} . These chains are linked to twice the number of boron-oxygen chains via common OH vertices to form three-layer sheets parallel to (100), which are linked into a single structure by Ca cations and hydrogen bonds.

Hydroboracite is a hydrated double borate of calcium and magnesium $\text{CaMgB}_6\text{O}_{11} \cdot 6\text{H}_2\text{O}$, which Petrova [1] first examined in 1958; the cell (monoclinic) has $a = 11.64$, $b = 6.62$, $c = 8.24$ Å, and $\beta = 102^\circ 54'$, the diffraction group being $2/mP/c$. A preliminary communication on the structure was published in 1962 [2].

We used needle crystals (elongated along \underline{c}) from the Mineralogical Museum of the Academy of Sciences; these could not be made spherical on account of the cleavage. The cell parameters (RKV camera, Cu K radiation) were found as $a = 11.71 \pm 0.03$, $b = 6.69 \pm 0.01$, $c = 8.20 \pm 0.02$ Å, $\beta = 102^\circ 40'$. The density is $d = 2.167$ [1], so the cell contains 2 formula units $\text{CaMgB}_6\text{O}_{11} \cdot 6\text{H}_2\text{O}$. Weissenberg patterns were recorded for the 0, 1, and 2 layer lines by rotation on \underline{c} and for the 0 and 1 layer lines by rotation on \underline{b} , both with MoK radiation. There were 146 finite F_{hk0}^2 , 260 F_{hk1}^2 , 216 F_{hk2}^2 , 183 F_{h0l}^2 , and 253 $\sqrt{F_{h1l}^2}$. The intensities were estimated from multiple exposures on the blackening scale (interval $\sqrt[4]{2}$) and were reduced to the absolute scale by Wilson's method [3]. The systematic absences

were examined as in [1]; they indicated Pc and $P2/c$ as the possible space groups. Tests for the piezoelectric effect gave a negative result, but the final decision in favor of group $C_{2h}^4 = P2/c$ was made while the structure was being interpreted by reference to the statistics of the F_{hk1}^2 [4].

The positions of the Ca and Mg were first found. There is an appreciable repeat $c' = c/2$ in the rotation pattern on \underline{c} , which indicates that the Ca and Mg atoms lie in twofold positions with similar x and y coordinates, but with z coordinates differing by $c/2$. The Patterson projections $P(u, v)$, $C_2(u, v)$, and $S_2(u, v)$ were constructed in order to test this. The strongest peak (at $1/2, 1/2$) in the $P(u, v)$ projection corresponded to a minimum at $1/2, 1/2$ in the weighted projection

$$C_2(u, v) = \int_0^1 P(u, v, w) \cos 4\pi w \, dw,$$

so the vector $[1/2, 1/2, 1/4]$ was identified as the Ca-Mg vector between pairs of Ca and Mg atoms that overlap

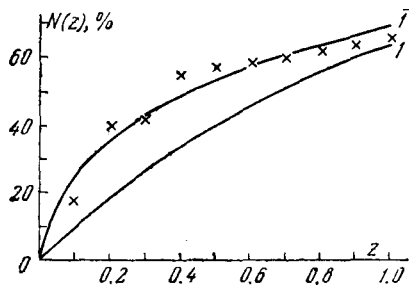


Fig. 1. Distribution of the intensities of hkl reflections compared with theoretical ones for symmetries 1 and $\bar{1}$.

in the xy projection. This, taken with group $P2/c$, indicates that one pair of cations lies at the centers of symmetry at 000 and $00\frac{1}{2}$ (we assumed that these atoms are always the more symmetrical Mg), the pair of Ca cations lying on the twofold axes at $\frac{1}{2}, y, \frac{1}{4}$ and $\frac{1}{2}, y, \frac{3}{4}$; the y coordinates are close to $\frac{1}{2}$. The statistics of the F_{hkl}^2 (Fig. 1) are quite unaffected by the Mg and nearly so by the Ca; this confirmed that the other atoms form a centrosymmetric array (group $P2/c$).

It was difficult to locate the light atoms from the Patterson syntheses on account of the prominent pseudocenters of symmetry at $\frac{1}{4}, \frac{1}{4}$ in the u, v projection and at $\frac{1}{4}, \frac{1}{8}$ in the u, w projection. These relate the Ca-O and Mg-O vectors, which are nominally distinct, but the heights of the peaks related by this pseudosymmetry were very similar, on account of overlap between vectors. Partial Fourier syntheses proved very valuable; these were computed from structure factors for indices of even type (syntheses of increased symmetry). In this case we at first took the pseudocenters as true centers of symmetry (or antisymmetry) and drew up projections for one-color and black-and-white symmetry [5-7]. First we used the F_{hko} with $h+k=2n$ and the F_{h0l} with $h+l/2=2n$, most of whose signs were clear, for the contributions from the Ca and Mg add up in these (in the initial calculation it was assumed that $y_{Ca} = \frac{1}{2}$; then $F_{Ca, Mg} = 2[f_{Mg} + (-1)^{h+k+l/2}f_{Ca}]$ for $l=2n$ and $F_{Ca, Mg} = 0$ for $l=2n+1$). Moreover, allowance could be made for some of the major peaks related by the pseudocenters in the Patterson syntheses, since one of each pair must undoubtedly correspond to the true position of the atom, and the contributions from either of the atoms so related are the same for structure factors having $h+k=2n$ (and correspondingly $h+l/2=2n$). However, these peaks had very little effect on the signs of the F_{hko} as defined by reference to the Ca and Mg, so the signs of the F_{h0l} for $h+l/2=2n$ were initially calculated only from the coordinates of the Ca and Mg.

These structure factors were used in series of difference syntheses $\Delta\sigma_{h+k=2n}(x, y)$ and $\Delta\sigma_{h+l/2=2n}(x, z)$, whose symmetries were respectively cmm and $c2(c' = c/2)$, in which the numbers of atoms were double the true ones (on account of the raised symmetry). The

contributions of the Ca and Mg were subtracted in the first stages; then the same was done for the other large peaks, which were taken initially as representing O atoms. Some peaks were too high and required a second subtraction, since they corresponded to atoms of the doubled set overlapping in the projections. On the other hand, the subtraction left hollows in other cases, so the corresponding peaks were taken as representing boron atoms in the next difference synthesis. This gave us the positions of double the number of all atoms (except O_1) related by the pseudocenters; moreover, the types could be distinguished. The result at this stage was characterized by $R_{hko} = 20\%$ for $h+k=2n$ and $R_{h0l} = 23\%$ for $h+l/2=2n$. Figure 2 illustrates the $\sigma_{h+k=2n}(x, y)$ synthesis as constructed from 81 F_{hko} with $h+k=2n$, the signs being calculated from the coordinates finally adopted (Table 1).

The true positions were deduced from those of the double set by constructing $\sigma_{h+k=2n+1}^0(x, y)$ and $\sigma_{h+l/2=2n+1}^0(x, z)$ (Fig. 3) for the $h+k=2n+1$ (and correspondingly $h+l/2=2n+1$) reflections of zero experimental intensity, the Fourier coefficients for these being $F_{Ca, Mg} = 2(f_{Ca} - f_{Mg})$. The pseudocenters became centers of antisymmetry in these syntheses, since the symmetry of the first projection was described by

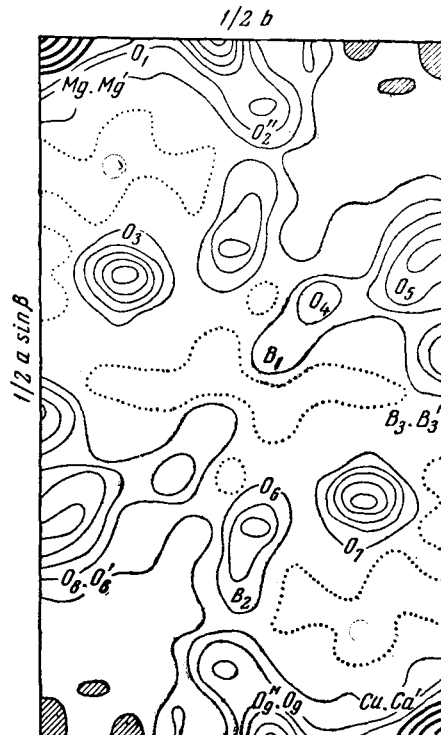


Fig. 2. Fourier synthesis $\sigma_{h+k=2n}(x, y)$ for hydroboracite. The thin lines are at intervals of $3 e/A^2$; the thick ones, $15 e/A^2$, the broken lines corresponding to hollows. The true positions of the atoms are shown.

TABLE 1. Coordinates of the Basal Atoms in Hydroboracite

Atom	x/a	y/b	z/c	Atom	x/a	y/b	z/c
Mg	0	0	0	O ₆	0.350±0.001	0.269±0.002	0.106
Ca	0,5	0.477	0.25	O ₇	0.328±0.001	0.387±0.003	0.819
O ₁ **	0	0.120±0.002	0.25	O ₈ **	0.355±0.001	0.027	0.895
O ₂ **	-0.049±0.001	0.278±0.001	-0.098	O ₉ **	0.509±0.001	0.283±0.001	-0.029
O ₃ **	0.168±0.002	0.092±0.001	0.035	B ₁	0.226±0.002	0.291±0.003	0.090
O ₄ **	0.190±0.001	0.340±0.003	0.246	B ₂	0.383±0.001	0.240±0.003	-0.051
O ₅ **	0.177±0.001	0.449±0.003	-0.031	B ₃	0.231±0.001	0.500	0.843

*O in OH.

**O in water molecule.

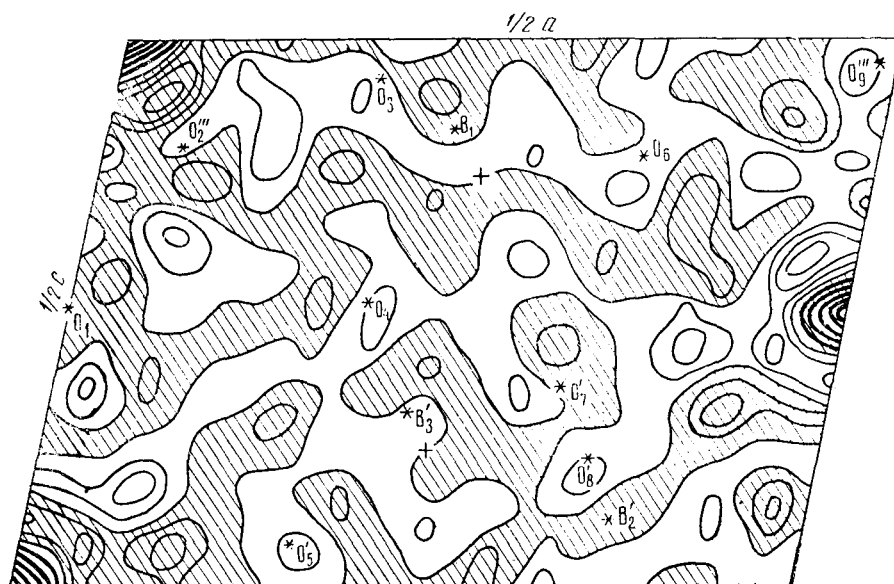


Fig. 3. Fourier synthesis $\sigma_{h+l/2}^0 = 2n+1(x, z)$ constructed from the zero reflections with $h + l/2 = 2n + 1$. The thin lines are at intervals of $0.5 e/A^2$; the thick ones, at $1 e/A^2$. The negative regions are hatched. The asterisks denote the true positions; the crosses correspond to centers of antisymmetry.

the black-and-white group p_2^1mm and the second by group p_2^2 (for $c' = c/2$) [5-7]. The contributions from the light atoms equal the sum of those from Ca and Mg for these reflections, so the positive regions in σ^0 must correspond to the true atoms, the negative ones related to them by the centers of antisymmetry being the false ones. The intensities were photographic, and the patterns had a background, so we could not be sure which F_{hkl} were exactly zero; we therefore used only values below the lowest entry on the blackening scale. Figure 4 shows curves for the background relative to $2(f_{Ca} - f_{Mg})$; in accordance with this we included reflections having $\sin \theta/\lambda$ such that the background was less than $2(f_{Ca} - f_{Mg})$.

The electron densities in σ^0 were extremely small (Fig. 3), but the selection of the position falling in the positive region gave the positions of most of the atoms correctly, apart from the two light atoms B₁ and B₂ (which lay in negative regions, together with O₁). The

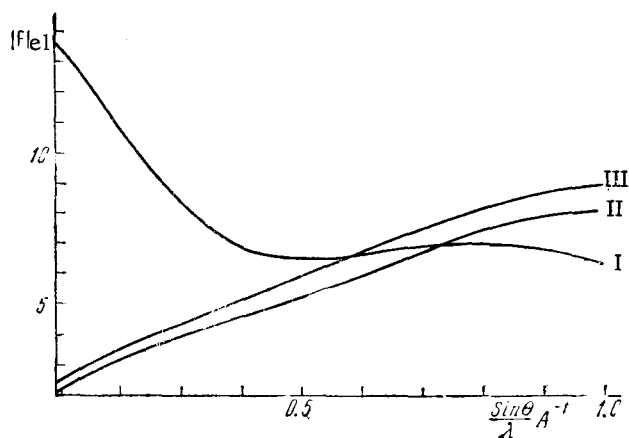


Fig. 4. Comparison of $2(f_{Ca} - f_{Mg})$ with the background intensity for $hk0$ and $h0l$ Weissenberg patterns: I) $2(f_{Ca} - f_{Mg})$; II) background curve for $hk0$; III) background for $h0l$.

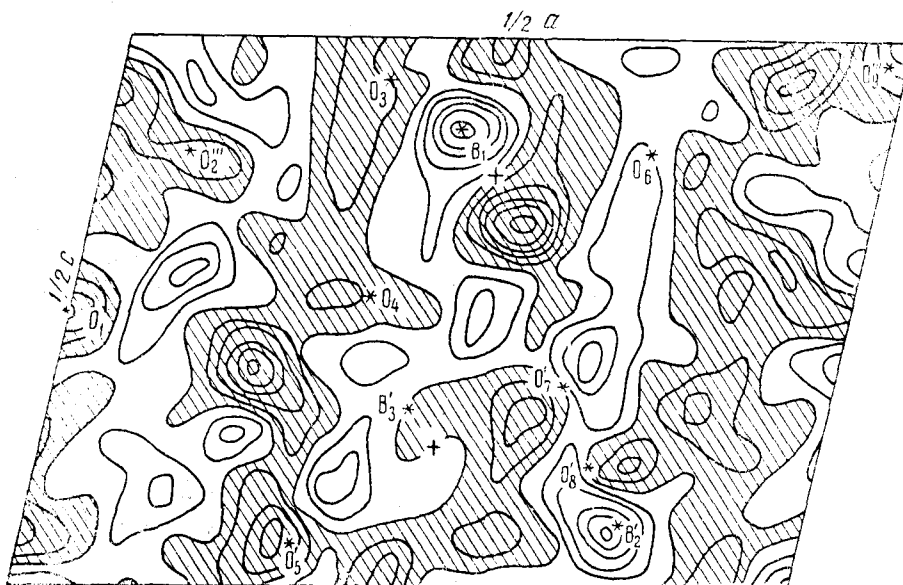


Fig. 5. Error synthesis $\Delta\sigma_{h+l/2=2n+1}(x, z)$; the contours are at intervals of $1 e/A^2$, the region of negative values being hatched. The asterisks denote the true positions of the atoms.

positions of B_1 and B_2 were deduced from error syntheses constructed from all F_{h0l} having $h + l/2 = 2n + 1$, the contributions from all definitely located atoms being subtracted (Fig. 5). The points corresponding to the positions chosen for B_1 and B_2 lay in highly negative regions, so the true positions were clearly those of the peaks related to these by the centers of antisymmetry.

There was a deep depression at $1/2, 1/2$ on $\Delta\sigma_{h+k=2n+1}(x, y)$ peaks along the line $x = 1/2$, which means that the Ca atoms overlapping in the xy projection must be displaced from the point $1/2, 1/2$ along the twofold axes. The next difference synthesis (from all F_{hk0}) was performed with subtraction of all located atoms, including the Ca, the y coordinate for the latter being the revised one; this gave the position of O_1 , which previously had been concealed by error waves (from the Ca). Subsequent difference syntheses gave the y coordinate of Ca more precisely; the Ca atoms actually do lie on the $1/2, y, 1/4$ and $1/2, \bar{y}, 3/4$ twofold axes.

Next we performed a machine cycle of refinement on ordinary $\alpha(x, y)$ and $\alpha(x, z)$ projections [Fig. 6 gives the final $\sigma(x, y)$ and $\sigma(x, z)$] and also on phase [8] weighted projections, which were constructed from the F_{hk1} , F_{hk2} , and F_{h1l} . Table 1 gives the coordinates of the basal atoms as averaged over all syntheses (from two-dimensional sets of F_{hk1}), as well as the mean errors of these. Tables 2-4 give the experimental and calculated F_{hk0} , F_{hk1} , and F_{h0l} . The result for all finite reflections, with allowance for isotropic temperature corrections, is

$$R_{hk0} = 10.3\% \left(\frac{\sin \theta}{\lambda} \leq 1.15 \text{ \AA}^{-1}, \right. \\ \left. B_{hk0} = 0.7 \text{ \AA}^2 \right),$$

$$R_{hk1} = 11.1\% \left(\frac{\sin \theta}{\lambda} \leq 1.15 \text{ \AA}^{-1}, B_{hk1} = 0.8 \text{ \AA}^2 \right),$$

$$R_{hk2} = 11.6\% \left(\frac{\sin \theta}{\lambda} \leq 1.05 \text{ \AA}^{-1}, B_{hk2} = 0.4 \text{ \AA}^2 \right),$$

$$R_{h0l} = 16.8\% \left(\frac{\sin \theta}{\lambda} \leq 1.15 \text{ \AA}^{-1}, B_{h0l} = 0.8 \text{ \AA}^2 \right),$$

$$R_{h1l} = 16.7\% \left(\frac{\sin \theta}{\lambda} \leq 1.10 \text{ \AA}^{-1}, B_{h1l} = 0.7 \text{ \AA}^2 \right).$$

R_{h0l} and R_{h1l} are larger on account of errors in I_{h0l} and I_{h1l} , which were determined by rotation on \underline{b} , which is perpendicular to the length of the crystal.

Figure 7 shows the main features of the structure; the most characteristic are the infinite boron-oxygen chains, which extend along \underline{c} and which resemble the chains in colemanite [10]. The basic element in each chain is a BO_3 triangle together with $BO_3(OH)$ and $BO_2(OH)_2$ tetrahedra, which are joined by common vertices into a ring with three nuclei $[B_3O_5(OH)_3]^{4-}$. The B-tetrahedra alternate with the B-triangles along the line of the chain; the second tetrahedra are merely attached at the side. The Mg atoms lie at centers of symmetry within octahedra made up each of four H_2O molecules and two OH groups. The Mg octahedra are linked via common H_2O vertices into $[Mg(OH)_2 \cdot 3H_2O]_n$ chains, which also extend along \underline{c} and which resemble the chains of octahedra found in UF_5 , sphene, and so on. The unit cell has two Mg octahedra with a mirror relation; each pair of Mg chains translationally identical along \underline{b} is linked [on both sides on (100)] to two $[B_3O_4(OH)_3]_n^{2n-}$ chains. These magnesium and boron-oxygen chains together make up three-layer sheets, which are parallel to (100) and which are linked into a single structure by columns of Ca polyhedra parallel to \underline{c} , as well as by hydrogen bonds. Each Ca atom is surrounded by eight oxygen

TABLE 2. Experimental and Calculated F_{hk0} for Hydroboracite. The F_i include a temperature factor $\exp \left[-0.7 \text{ \AA}^2 \left(\frac{\sin \phi}{\lambda} \right)^2 \right]$. $R_{hk0} = 10.3\%$
 from the $F_0 \neq 0$; $\left(\frac{\sin \phi}{\lambda} \leq 1.15 \text{ \AA}^{-1} \right)$

$h \backslash k$	0	1	2	3	4	5	6	7	8	9	10	11	12
0	— +398	— -46.8	15.4 +14.5	53.1 +44.4	66.0 +59.3	38.2 -37.9	<5.0 +2.9	18.6 +15.0	23.5 +22.9	<6.5 -7.1	<7.1 +8.6	14.5 +14.4	<8.0 -2.6
1	— -18.2	53.7 +51.6	5.9 +5.7	16.1 +13.6	34.3 -29.1	7.8 +6.6	5.2 +2.6	12.0 +11.4	<6.0 -4.6	17.3 +17.0	<7.1 +3.4	<7.6 +5.6	<8.0 +4.5
2	11.8 +12.0	21.4 +22.4	14.6 -6.9	12.1 -9.3	44.5 +43.0	7.3 -8.4	10.9 +9.1	18.2 +16.7	10.1 +11.6	<6.6 -1.4	<7.2 +4.5	<7.6 +5.1	<8.1 -4.3
3	11.2 -12.8	78.6 +83.0	23.7 -22.2	57.9 +52.5	9.1 -8.0	52.4 +52.4	7.6 -7.9	19.0 +21.2	20.9 +21.7	<6.6 -5.0	<7.3 +2.5	<7.6 -3.5	<8.1 -0.9
4	31.3 +31.3	33.6 -34.1	16.5 +17.1	14.0 -15.7	29.6 +25.8	26.6 -28.8	33.2 +29.8	10.3 -7.3	<6.2 +7.0	<6.7 -6.1	12.6 +14.5	<7.7 +1.6	<8.1 -3.1
5	30.1 +35.2	40.6 +44.6	8.9 +8.7	20.7 +21.8	5.2 -5.5	9.5 +8.2	5.4 +3.5	<5.8 +5.5	<6.3 +1.0	21.2 +22.4	<7.4 -3.5	<7.7 +1.3	10.1 +8.3
6	119 +134	7.7 -7.0	36.2 +39.6	15.6 +15.5	9.0 +11.0	5.3 -5.6	<5.5 +2.5	9.6 +7.8	8.0 +10.5	<7.0 +5.8	<7.5 +2.5	12.0 +13.7	<8.1 -3.1
7	68.2 -68.5	42.7 +48.7	17.5 +19.6	5.2 -5.3	37.8 -39.3	28.3 +27.9	<5.6 -3.2	<6.1 +0.3	<6.6 -4.3	23.8 +22.1	<7.6 +1.4	<7.9 -0.8	<8.1 +5.4
8	16.2 +23.0	13.4 +16.5	19.2 +19.4	11.0 -11.1	41.3 +44.6	7.0 -6.9	14.3 +14.4	6.4 +5.9	16.5 +17.2	<7.2 -4.6	<7.6 +7.9	<8.0 -4.2	
9	15.1 -16.4	21.8 +24.0	<4.9 +6.6	25.3 +23.8	8.5 -11.0	23.2 +25.7	13.7 +12.0	8.0 +7.8	11.4 +10.3	<7.4 -3.6	8.5 +8.7	<8.1 -7.3	
10	15.1 +13.9	13.3 -14.1	15.7 +17.5	<5.3 -9.2	<5.5 +2.4	<5.8 -2.3	18.0 +18.0	<6.6 -5.6	<7.1 +3.8	11.8 +12.1	<7.8 +0.2	<8.1 -2.2	
11	<5.2 -0.8	34.7 +38.0	9.1 +11.6	14.2 +16.3	13.1 -12.4	20.0 +21.2	<6.4 -1.2	<6.8 +4.7	<7.3 -3.6	21.8 +26.3	8.4 -10.6		
12	34.4 +38.0	8.1 -7.0	29.2 +30.9	8.6 -7.9	<6.0 +2.6	<6.3 -6.7	<6.7 +4.6	<7.1 +0.1	<7.5 +7.3	<7.7 +1.2	<8.1 +8.2		
13	24.8 -14.5	19.6 +20.7	<5.9 +3.0	<6.1 -3.4	7.2 -7.3	9.9 +9.1	<7.0 -3.2	<7.4 -0.9	<7.7 +4.2	<7.9 +7.2	8.8 +8.0		

TABLE 3. Experimental and Calculated F_{h0l} for Hydroboracite. The F_c include a temperature factor $\exp \left[-0.8 A^2 \left(\frac{\sin \phi}{\lambda} \right)^2 \right]$. R_{h0l}
 = 16.8% from the $F_0 \neq 0$; $\left(\frac{\sin \phi}{\lambda} \ll 1.15 A^{-1} \right)$

$h \backslash l$	18	16	14	12	10	8	6	4	2	0	2	4	6	8	10	12	14	16	18
0	<9.0 -6.1	<8.9 -0.1	23.1 -28.7	13.4 +14.7	<6.9 -6.3	23.1 +29.7	26.1 -28.2	34.4 +48.4	24.8 +37.0	— +398	24.8 +37.0	34.4 +48.4	26.1 -23.2	23.1 +29.7	<6.9 -6.3	13.4 +14.7	23.1 -28.7	<8.9 -0.1	<9.0 -6.1
1	<9.0 +1.1	<9.0 -3.5	9.8 +12.4	<7.8 +3.2	13.6 +16.6	16.0 -15.1	<4.8 +6.5	32.0 +35.5	8.3 +14.8	— -18.2	33.4 +38.8	13.9 -16.3	15.9 +22.4	14.2 +19.3	<7.0 +6.3	<7.9 +1.3	<8.7 +6.4	<8.9 -6.4	<9.0 +1.9
2	<9.0 -2.6	<9.0 +4.1	<8.5 -2.6	9.2 +10.6	7.1 -7.3	18.3 +21.7	<4.8 -3.5	42.5 +47.9	42.5 +47.0	15.3 +11.9	31.8 -33.7	31.8 +39.8	14.2 -19.1	20.9 +27.1	<7.1 +3.0	7.7 +5.2	<8.7 -0.1	9.8 +11.1	<9.0 -2.9
3	9.1 +12.3	<9.0 +4.1	8.6 +11.6	<7.6 +4.9	33.4 +39.0	<5.8 -2.9	<4.8 +4.6	72.8 -94.8	6.5 +9.9	13.1 -12.8	22.2 -17.8	56.0 -66.1	13.2 +15.8	12.4 -12.5	24.2 +32.6	<8.2 -1.0	<8.7 +3.9	<9.0 +4.6	11.5 +13.4
4	9.2 -12.7	<9.0 +6.6	<8.5 +2.8	18.6 +22.3	7.4 -8.3	19.8 +23.8	10.8 -16.3	72.6 +83.6	25.3 -22.9	42.8 +31.8	31.1 -26.2	33.1 +34.9	6.9 +9.4	20.3 +25.3	12.4 -13.3	17.5 +18.6	<8.8 +0.6	<9.0 +4.6	
5	<9.0 +3.4	<9.0 -4.7	<8.5 +6.1	<7.7 +9.7	<6.8 -1.9	<5.9 -6.0	<5.1 +5.4	20.9 +22.3	67.0 +66.1	39.7 +35.2	8.9 +5.7	<4.8 -1.5	<5.7 +1.1	7.8 +11.4	<7.6 +6.1	8.1 -8.9	<8.9 +2.0		
6	<9.0 -7.5	<9.0 +6.2	18.6 -19.7	10.1 +11.4	10.6 -11.9	<6.0 +8.5	— -19.1	54.6 +63.7	20.9 +18.3	137 +134.0	<4.4 +0.3	54.0 +52.8	<5.9 +4.8	34.5 +39.6	<7.7 -2.7	<8.5 +0.6	16.3 -22.3		
7	<9.0 -13.0	<9.0 -1.0	19.8 +19.5	14.3 -12.2	8.7 +10.0	12.8 -10.6	36.1 +36.6	43.5 +43.5	39.8 +30.8	79.9 -67.8	11.8 +7.6	<5.4 +0.9	29.8 +30.5	8.3 -8.6	<7.9 -2.5	<8.6 -2.9	11.5 +12.2		
8	<9.0 -0.7	<9.0 +4.4	<8.5 +1.1	<7.8 +10.3	9.8 -10.6	23.4 +24.2	6.6 -8.7	<5.0 +3.9	11.3 +13.6	20.2 +22.8	<5.1 -6.1	33.0 +25.9	6.4 -4.8	10.2 +11.1	<8.0 -1.4	<8.6 +5.6	<8.9 +0.4		
9	<9.0 +10.7	<9.0 +7.2	9.8 +13.8	19.2 +18.7	24.6 +26.0	<6.4 -1.5	30.3 +26.7	29.2 -25.5	24.6 -7.4	18.8 -16.2	12.3 -14.0	34.8 -31.5	12.7 +12.8	<7.5 -5.5	13.4 +15.2	<8.7 +1.6	<9.0 +8.0		

TABLE 4. Experimental and Calculated F_{hk1} for Hydroboracite. The F_t include a temperature factor $\exp \left[-0.8 A^2 \left(\frac{\sin \phi}{\lambda} \right)^2 \right]$. $R_{hk1} = 11.1\%$ from the $F_o \neq 0$; $\left(\frac{\sin \phi}{\lambda} \ll 1.15 \text{ \AA}^{-1} \right)$.

$\begin{matrix} k \\ h \end{matrix}$	1	2	3	4	5	6	7	8	9	10	11	12	13	14
24					7.1 -6.6	7.1 +5.2								
21	<6.5 +5.3	7.8 -6.4	<6.5 +0.9	<6.5 -4.5	<6.6 +7.9	9.0 -8.2				9.0 -8.3				
20	<6.4 -5.1	<6.4 +1.7	7.9 -6.5	<6.4 +0.5	<6.5 -1.6	<6.5 +4.6								
19	<6.2 +1.6	<6.3 -6.6	<6.3 -5.5	<6.4 +3.2	<6.4 +2.8	<6.5 -1.6	<6.5 +8.0		7.9 +6.3					
18	<6.0 -4.6	<6.1 -3.6	<6.2 -2.3	<6.2 -0.8	15.7 -13.4	14.3 +14.5	<6.5 -7.7				7.2 -6.5			
17	<5.8 -0.3	<5.8 +0.4	<6.0 +3.4	<6.1 -0.2	10.0 +7.6	10.6 -6.1	9.1 +8.7	<6.5 -4.6						
16	<5.5 -3.5	6.2 +7.2	<5.8 +1.4	<5.8 +2.6	<6.0 +5.6	<6.2 +1.0	<6.4 -3.1	<6.5 +4.8	<6.5 -6.6					
15	<5.3 -0.3	6.1 -7.4	5.7 +8.9	14.2 -15.1	7.8 +5.9	<6.1 -2.9	<6.3 +0.7	9.1 -10.3	<6.5 +1.2	7.2 -7.1				
14	18.6 -19.9	<5.1 +4.0	<5.2 +2.1	<5.4 +1.7	12.4 -12.9	19.2 +18.1	<6.1 +5.3	<6.3 +2.3	<6.5 -1.8	8.2 +11.6	8.2 -7.5			
13	<4.8 +0.9	10.7 -9.4	9.7 -11.6	<5.2 -0.2	<5.4 +1.3	<5.7 +0.6	12.8 +10.0	<6.2 -4.5	9.9 +9.7	<6.5 -2.6	<6.5 +2.7			6.5 -5.9
12	9.2 -11.3	<4.6 -5.6	<4.8 -0.7	<5.0 -1.2	17.7 -19.7	17.7 +18.2	7.9 -8.3	<6.0 +1.7	9.4 -10.3	<6.5 +5.8	<6.5 -5.1			

TABLE 4 (continued)

$\begin{matrix} k \\ h \end{matrix}$	1	2	3	4	5	6	7	8	9	10	11	12	13	14
11	$\begin{matrix} <4.2 \\ -5.4 \end{matrix}$	$\begin{matrix} <4.4 \\ +4.3 \end{matrix}$	$\begin{matrix} 10.9 \\ +12.1 \end{matrix}$	$\begin{matrix} <4.8 \\ -3.7 \end{matrix}$	$\begin{matrix} 18.4 \\ +18.2 \end{matrix}$	$\begin{matrix} 11.3 \\ -9.6 \end{matrix}$	$\begin{matrix} 14.7 \\ +14.4 \end{matrix}$	$\begin{matrix} <5.9 \\ -2.2 \end{matrix}$	$\begin{matrix} <6.2 \\ +3.4 \end{matrix}$	$\begin{matrix} <6.4 \\ -6.9 \end{matrix}$	$\begin{matrix} 7.4 \\ +8.5 \end{matrix}$			
10	$\begin{matrix} 8.4 \\ -8.2 \end{matrix}$	$\begin{matrix} 14.3 \\ +15.8 \end{matrix}$	$\begin{matrix} <4.4 \\ -1.5 \end{matrix}$	$\begin{matrix} <4.5 \\ -6.0 \end{matrix}$	$\begin{matrix} <4.8 \\ +8.8 \end{matrix}$	$\begin{matrix} 6.7 \\ +5.2 \end{matrix}$	$\begin{matrix} 12.8 \\ -11.6 \end{matrix}$	$\begin{matrix} <5.8 \\ -3.0 \end{matrix}$	$\begin{matrix} 7.3 \\ -7.1 \end{matrix}$	$\begin{matrix} <6.4 \\ +5.1 \end{matrix}$	$\begin{matrix} 11.9 \\ -11.9 \end{matrix}$			$\begin{matrix} 7.7 \\ +7.0 \end{matrix}$
9	$\begin{matrix} 5.2 \\ -7.0 \end{matrix}$	$\begin{matrix} 15.6 \\ -17.8 \end{matrix}$	$\begin{matrix} 24.5 \\ +25.6 \end{matrix}$	$\begin{matrix} 15.1 \\ -16.6 \end{matrix}$	$\begin{matrix} <4.6 \\ -2.8 \end{matrix}$	$\begin{matrix} <5.0 \\ 0.0 \end{matrix}$	$\begin{matrix} 11.8 \\ +9.1 \end{matrix}$	$\begin{matrix} 15.3 \\ -14.4 \end{matrix}$	$\begin{matrix} <6.0 \\ +2.0 \end{matrix}$	$\begin{matrix} 7.9 \\ -8.8 \end{matrix}$	$\begin{matrix} 7.7 \\ +5.1 \end{matrix}$	$\begin{matrix} 7.2 \\ -8.5 \end{matrix}$		
8	$\begin{matrix} <3.6 \\ +2.8 \end{matrix}$	$\begin{matrix} <5.1 \\ -7.4 \end{matrix}$	$\begin{matrix} 21.8 \\ -23.5 \end{matrix}$	$\begin{matrix} 25.2 \\ +23.6 \end{matrix}$	$\begin{matrix} 8.2 \\ -9.5 \end{matrix}$	$\begin{matrix} 17.3 \\ +17.4 \end{matrix}$	$\begin{matrix} <5.1 \\ +2.7 \end{matrix}$	$\begin{matrix} 16.2 \\ +15.4 \end{matrix}$	$\begin{matrix} <5.9 \\ -1.4 \end{matrix}$	$\begin{matrix} 7.8 \\ +10.0 \end{matrix}$	$\begin{matrix} <6.5 \\ -7.2 \end{matrix}$	$\begin{matrix} 7.2 \\ +7.6 \end{matrix}$		
7	$\begin{matrix} 6.8 \\ +7.8 \end{matrix}$	$\begin{matrix} 19.0 \\ -20.4 \end{matrix}$	$\begin{matrix} 33.9 \\ -40.2 \end{matrix}$	$\begin{matrix} <4.0 \\ +2.1 \end{matrix}$	$\begin{matrix} 5.5 \\ +6.3 \end{matrix}$	$\begin{matrix} 12.7 \\ -12.4 \end{matrix}$	$\begin{matrix} 10.0 \\ +9.1 \end{matrix}$	$\begin{matrix} <5.3 \\ -2.4 \end{matrix}$	$\begin{matrix} 6.4 \\ +7.2 \end{matrix}$	$\begin{matrix} 8.7 \\ -9.9 \end{matrix}$	$\begin{matrix} <6.4 \\ +1.2 \end{matrix}$	$\begin{matrix} <6.5 \\ -7.0 \end{matrix}$		
6	$\begin{matrix} 25.7 \\ -27.9 \end{matrix}$	$\begin{matrix} 6.0 \\ -7.3 \end{matrix}$	$\begin{matrix} <3.5 \\ +4.1 \end{matrix}$	$\begin{matrix} <3.8 \\ -2.3 \end{matrix}$	$\begin{matrix} 14.8 \\ -17.4 \end{matrix}$	$\begin{matrix} 20.4 \\ +19.8 \end{matrix}$	$\begin{matrix} 10.4 \\ -9.2 \end{matrix}$	$\begin{matrix} 15.7 \\ +15.4 \end{matrix}$	$\begin{matrix} 14.1 \\ -13.1 \end{matrix}$	$\begin{matrix} <6.0 \\ +1.5 \end{matrix}$	$\begin{matrix} <6.4 \\ -0.6 \end{matrix}$	$\begin{matrix} <6.5 \\ +0.4 \end{matrix}$		
5	$\begin{matrix} 21.8 \\ +23.4 \end{matrix}$	$\begin{matrix} 7.3 \\ +6.7 \end{matrix}$	$\begin{matrix} <3.3 \\ +1.8 \end{matrix}$	$\begin{matrix} 9.9 \\ -9.6 \end{matrix}$	$\begin{matrix} 51.2 \\ +48.4 \end{matrix}$	$\begin{matrix} 15.7 \\ -14.7 \end{matrix}$	$\begin{matrix} 6.9 \\ +6.2 \end{matrix}$	$\begin{matrix} <5.1 \\ -2.7 \end{matrix}$	$\begin{matrix} 12.2 \\ +13.3 \end{matrix}$	$\begin{matrix} 9.5 \\ -11.7 \end{matrix}$	$\begin{matrix} <6.4 \\ +6.0 \end{matrix}$	$\begin{matrix} <6.5 \\ +1.5 \end{matrix}$		
4	$\begin{matrix} 7.3 \\ +11.1 \end{matrix}$	$\begin{matrix} 4.8 \\ +6.4 \end{matrix}$	$\begin{matrix} 17.0 \\ -17.4 \end{matrix}$	$\begin{matrix} 10.4 \\ +10.6 \end{matrix}$	$\begin{matrix} <3.8 \\ +4.9 \end{matrix}$	$\begin{matrix} 10.0 \\ -12.3 \end{matrix}$	$\begin{matrix} 11.3 \\ -10.3 \end{matrix}$	$\begin{matrix} <5.1 \\ +1.0 \end{matrix}$	$\begin{matrix} 15.6 \\ -17.2 \end{matrix}$	$\begin{matrix} <5.9 \\ -1.4 \end{matrix}$	$\begin{matrix} 9.8 \\ -12.6 \end{matrix}$	$\begin{matrix} 8.8 \\ +10.0 \end{matrix}$		
3	$\begin{matrix} 40.0 \\ +41.7 \end{matrix}$	$\begin{matrix} 58.8 \\ -55.9 \end{matrix}$	$\begin{matrix} 22.8 \\ +22.1 \end{matrix}$	$\begin{matrix} 7.0 \\ +8.1 \end{matrix}$	$\begin{matrix} <3.7 \\ +1.6 \end{matrix}$	$\begin{matrix} <4.2 \\ -5.9 \end{matrix}$	$\begin{matrix} 16.3 \\ +16.2 \end{matrix}$	$\begin{matrix} <5.0 \\ -4.6 \end{matrix}$	$\begin{matrix} <5.4 \\ +3.9 \end{matrix}$	$\begin{matrix} 13.6 \\ -12.8 \end{matrix}$	$\begin{matrix} 9.7 \\ +11.1 \end{matrix}$	$\begin{matrix} <6.5 \\ -4.9 \end{matrix}$		
2	$\begin{matrix} 47.0 \\ +50.1 \end{matrix}$	$\begin{matrix} 27.2 \\ -26.2 \end{matrix}$	$\begin{matrix} 88.8 \\ -79.0 \end{matrix}$	$\begin{matrix} 47.8 \\ +42.7 \end{matrix}$	$\begin{matrix} <3.7 \\ -0.2 \end{matrix}$	$\begin{matrix} 19.0 \\ +16.5 \end{matrix}$	$\begin{matrix} 12.0 \\ -10.6 \end{matrix}$	$\begin{matrix} 23.3 \\ +24.7 \end{matrix}$	$\begin{matrix} <5.4 \\ +0.1 \end{matrix}$	$\begin{matrix} <5.9 \\ +5.4 \end{matrix}$	$\begin{matrix} 8.5 \\ -8.9 \end{matrix}$	$\begin{matrix} 8.7 \\ +8.9 \end{matrix}$	$\begin{matrix} <6.5 \\ -2.8 \end{matrix}$	
1	$\begin{matrix} 75.4 \\ -66.5 \end{matrix}$	$\begin{matrix} 16.5 \\ -11.4 \end{matrix}$	$\begin{matrix} 46.2 \\ -44.0 \end{matrix}$	$\begin{matrix} 20.6 \\ -21.1 \end{matrix}$	$\begin{matrix} <3.6 \\ -1.4 \end{matrix}$	$\begin{matrix} 13.2 \\ -12.2 \end{matrix}$	$\begin{matrix} 13.3 \\ +13.6 \end{matrix}$	$\begin{matrix} 7.5 \\ -6.4 \end{matrix}$	$\begin{matrix} <5.3 \\ +4.2 \end{matrix}$	$\begin{matrix} 11.4 \\ -12.3 \end{matrix}$	$\begin{matrix} <6.2 \\ +1.6 \end{matrix}$	$\begin{matrix} 8.0 \\ -8.6 \end{matrix}$	$\begin{matrix} <6.5 \\ +1.0 \end{matrix}$	$\begin{matrix} 7.8 \\ -9.4 \end{matrix}$
0	$\begin{matrix} 20.8 \\ -20.1 \end{matrix}$	$\begin{matrix} 7.1 \\ -7.3 \end{matrix}$	$\begin{matrix} <2.7 \\ -1.7 \end{matrix}$	$\begin{matrix} <3.2 \\ -4.4 \end{matrix}$	$\begin{matrix} 5.9 \\ +5.0 \end{matrix}$	$\begin{matrix} 24.9 \\ +24.3 \end{matrix}$	$\begin{matrix} 11.5 \\ -12.8 \end{matrix}$	$\begin{matrix} 19.4 \\ +21.7 \end{matrix}$	$\begin{matrix} 6.2 \\ -6.8 \end{matrix}$	$\begin{matrix} <5.8 \\ +4.6 \end{matrix}$	$\begin{matrix} <6.2 \\ -0.1 \end{matrix}$	$\begin{matrix} <6.4 \\ +2.7 \end{matrix}$	$\begin{matrix} <6.5 \\ -4.7 \end{matrix}$	$\begin{matrix} 7.5 \\ +8.7 \end{matrix}$

TABLE 4 (continued)

$h \backslash k$	1	2	3	4	5	6	7	8	9	10	11	12	13	14
$\bar{1}$	53.0 +52.4	20.7 -16.6	12.4 +6.2	8.0 -8.5	51.1 +46.5	27.4 -25.1	9.9 +9.0	6.9 -6.3	8.8 +8.4	14.7 -15.2	8.7 +5.8	<6.4 +0.1	<6.5 +4.0	
$\bar{2}$	6.9 -5.5	<2.3 +0.2	3.5 -2.1	20.8 +20.4	20.0 -17.3	6.2 -9.0	<4.5 +1.0	7.9 -4.9	22.0 -22.7	<5.9 +3.1	11.4 -12.6	9.5 +8.9	<6.5 -7.5	
$\bar{3}$	7.6 +12.3	27.8 -29.7	37.2 +34.1	<3.3 -4.7	<3.7 +2.9	19.9 +20.8	10.9 +11.9	15.2 -15.1	13.2 +16.2	<5.9 -0.9	<6.2 +4.5	<6.4 -8.6	10.2 +12.5	
$\bar{4}$	23.7 -25.3	4.8 -5.3	42.7 -44.3	12.6 +12.5	17.7 -17.9	21.3 +22.5	10.6 -12.2	15.5 +17.8	5.7 -6.4	<5.9 +3.9	<6.2 -8.8	<6.4 +3.7		
$\bar{5}$	78.5 -86.7	9.0 +11.5	7.0 -7.4	34.9 -35.3	<3.9 0.0	<4.4 -2.4	16.0 +18.2	13.2 -12.0	<5.5 +3.3	<5.9 -3.2	<6.3 +3.0	10.8 -14.0		
$\bar{6}$	<2.9 +0.5	5.0 -8.0	<3.4 +0.1	<3.7 +2.0	<4.1 +8.2	18.3 +19.1	<4.8 -5.8	17.6 +18.5	6.7 -4.9	7.1 +7.7	<6.3 0.0	<6.5 +2.9		6.7 +10.4
$\bar{7}$	<3.2 -1.7	17.5 -16.9	26.4 +31.7	14.6 -17.3	5.1 +6.8	12.0 -11.5	12.1 +13.7	17.9 -21.0	<5.7 +3.4	8.9 -10.1	<6.3 -0.2	<6.5 -3.3		
$\bar{8}$	10.2 -15.2	10.0 +13.0	<3.8 +5.2	6.0 +7.0	13.8 -14.5	11.9 +13.6	<5.0 -0.9	11.6 -13.8	9.2 -10.5	12.9 +13.5	15.2 -16.3	<6.5 +4.3		
$\bar{9}$	6.8 -8.2	4.1 -4.5	18.1 +18.7	5.6 -6.0	<4.5 +2.4	11.2 +14.9	10.1 +9.2	9.7 -7.8	8.1 +11.3	<6.2 -2.4	<6.4 +6.3		10.2 +10.7	
$\bar{10}$	7.6 -11.1	4.1 -3.9	26.6 -27.5	8.2 +7.3	10.8 -11.4	<5.0 +5.8	13.0 -12.3	17.9 +19.7	10.4 -12.8	<6.3 -2.8	<6.5 -2.3			
$\bar{11}$	18.6 -23.4	<4.3 +3.7	5.4 -4.7	15.2 -18.6	10.2 +10.2	<5.1 -0.7	14.9 +15.3	8.8 -8.6	6.8 +7.3	<6.4 +1.2	<6.5 +2.4	9.3 -10.1		
$\bar{12}$	<4.4 +3.8	9.1 -9.5	<4.6 +1.2	6.5 +5.8	<5.1 -0.1	7.1 +8.5	<5.7 -1.4	12.8 +12.9	6.8 -3.3	<6.4 +2.2	<6.5 -3.0			

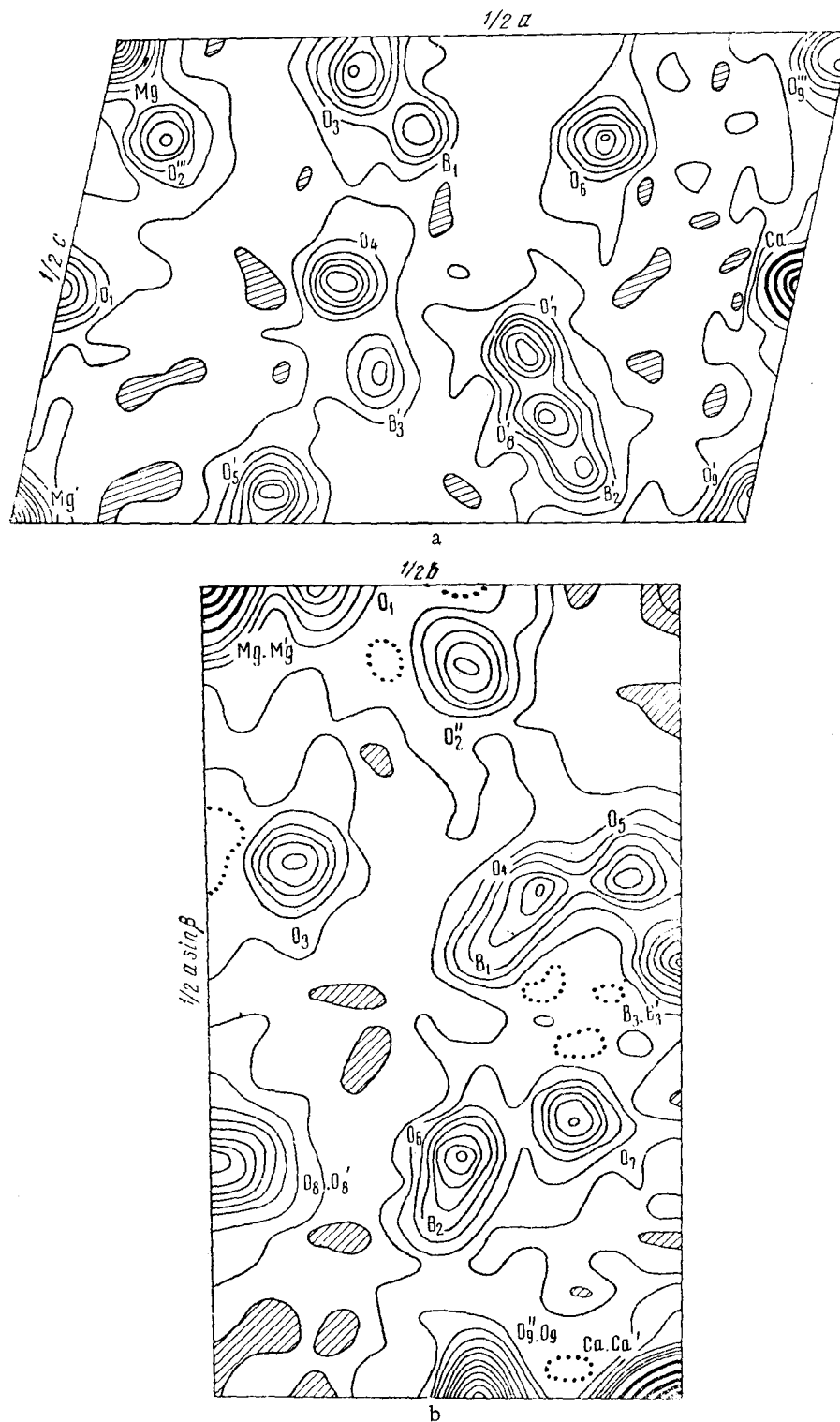


Fig. 6. Electron-density projections for hydroboracite: a) $\sigma(x, z)$; b) $\sigma(x, y)$. The thin lines are at intervals of $3 e/A^2$, the thick ones, $15 e/A^2$, the broken lines corresponding to hollows. A single prime denotes atoms related to the basal ones by a glide plane; two primes, ones so related by a twofold rotation axis; three, by a center of symmetry.

atoms, which form a 12-faced figure with triangular faces (Fig. 8). A quarter of the vertices have five faces

meeting; another quarter, four. A similar Ca polyhedron is found in colemanite [10] and also in kainosite [9]

TABLE 5. Interatomic Distances (A) and Bond Angles in Hydroboracite

B ₁ -Tetrahedron		B ₂ -Tetrahedron		B ₃ -Triangle	
B ₁ —O ₃ [*]	1.51	B ₂ —O ₆	1.44	B ₃ —O ₄ '	1.36
B ₁ —O ₄	1.47	B ₂ —O ₇	1.49	B ₃ —O ₅	1.37
B ₁ —O ₅	1.48	B ₂ —O ₈ [*]	1.51	B ₃ —O ₇	1.41
B ₁ —O ₆	1.44	B ₂ —O ₉ [*]	1.48	Mean	1.38
Mean	1.47	Mean	1.48	O ₅ —O ₄ '	2.34
O ₃ [*] —O ₄	2.37	O ₆ —O ₇	2.44	O ₅ —O ₇	2.40
O ₃ [*] —O ₅	2.46	O ₆ —O ₈ [*]	2.38	O ₄ '—O ₇	2.43
O ₃ [*] —O ₆	2.40	O ₆ —O ₉ [*]	2.37	Mean	2.39
O ₄ —O ₅	2.36	O ₇ —O ₈ [*]	2.49	O ₄ '—B ₃ —O ₅	118.0°
O ₄ —O ₆	2.45	O ₇ —O ₉ [*]	2.32	O ₄ '—B ₃ —O ₇	122.4°
O ₅ —O ₆	2.41	O ₈ [*] —O ₉ [*]	2.47	O ₅ —B ₃ —O ₇	119.3°
Mean	2.41	Mean	2.41	Sum	359.7°
O ₃ [*] —B ₁ —O ₄	105.4°	O ₆ —B ₂ —O ₇	112.5°	Ca-Polyhedron	
O ₃ [*] —B ₁ —O ₅	110.5°	O ₆ —B ₂ —O ₈ [*]	107.4°	Ca—O ₆	2.35
O ₃ [*] —B ₁ —O ₆	108.8°	O ₆ —B ₂ —O ₉ [*]	108.5°	Ca—O ₇	2.39
O ₄ —B ₁ —O ₅	106.1°	O ₇ —B ₂ —O ₈ [*]	112.3°	Ca—O ₉ [*]	2.41
O ₄ —B ₁ —O ₆	114.8°	O ₇ —B ₂ —O ₉ [*]	102.6°	Ca—O ₉ [*]	2.65
O ₅ —B ₁ —O ₆	111.4°	O ₈ [*] —B ₂ —O ₉ [*]	111.5°		
Mean	109.5°	Mean	109.1°		
		Mg-Octahedron			
Mg—O ₁ ^{**}	2.20	O ₁ ^{**} —O ₂ ^{**}	2.98	O ₁ ^{**} —O ₃ ^{***}	3.05
Mg—O ₂ ^{**}	2.06	O ₁ ^{**} —O ₃ [*]	2.92	O ₂ ^{**} —O ₃ [*]	2.83
Mg—O ₃ [*]	2.02	O ₁ ^{**} —O ₉ ^{***}	3.05	O ₂ ^{**} —O ₃ ^{***}	2.94

*O in OH.

**O in H₂O.

TABLE 6. Balance of Valencies in Hydroboracite

Anions, number of	Cations, number of					Sum of valencies
	B ₁ (4)	B ₂ (4)	B ₃ (4)	Mg (2)	Ca (2)	
O ₁ ^{**} (2)				2/6 × 2		0.67
O ₂ ^{**} (4)				2/6		0.33
O ₃ [*] (4)	3/4			2/6		1.08
O ₄ (4)	3/4		3/3			1.75
O ₅ (4)	3/4		3/3			1.75
O ₆ (4)	3/4	3/4			2/8	1.75
O ₇ (4)		3/4	3/3		2/8	2.00
O ₈ [*] (4)		3/4				0.75
O ₉ [*] (4)		3/4			2/8 × 2	1.25

*O in OH.

**O in water molecule.

8. I. M. Rumanova, *Kristallografiya*, 3, 6, 664 (1958)
[Soviet Physics - Crystallography, Vol. 3, p. 672].
9. G. F. Volodina, I. M. Rumanova, and N. V. Belov, *Dokl. AN SSSR*, 149, 1, 173 (1963).
10. C. L. Christ, J. R. Clark, and H. T. J. Evans, *Acta crystallogr.*, 11, 11, 761 (1958).
11. N. Morimoto, *Mineral. J. Japan*, 2, 1, 1 (1956).

All abbreviations of periodicals in the above bibliography are letter-by-letter transliterations of the abbreviations as given in the original Russian journal. *Some or all of this periodical literature may well be available in English translation.* A complete list of the cover-to-cover English translations appears at the back of this issue.